Synthesis and Characterization of Donor–Bridge–Acceptor Alternating Copolymers Containing Perylene Diimide Units and Their Application to Photovoltaic Cells

MAO-CHUAN YUAN, MING-HSIN SU, MAO-YUAN CHIU, KUNG-HWA WEI

Department of Materials Science and Engineering, National Chiao Tung University, 300 Hsinchu, Taiwan, Republic of China

Received 16 October 2009; accepted 14 December 2009
DOI: 10.1002/pola.23889
Published online in Wiley InterScience (www.interscience.wiley.com).

ABSTRACT: We have used Suzuki coupling to prepare a series of alternating copolymers featuring coplanar cyclopentadithiophene and hole-transporting carbazole units. We observed quenching in the photoluminescence spectra of our polymers after incorporating pendent electron-deficient perylene diimide (**PDI**) moieties on the side chains, indicating more efficient photoinduced electron transfer. Electrochemical measurements revealed that the **PDI**-containing copolymers displayed reasonable and sufficient offsets of the energy levels of their lowest unoccupied molecular orbitals for efficient charge dissociation. The performance of bulk heterojunction photovoltaic cells incorporating the copolymer/[6,6]-phenyl-C_{61}-butyric acid methyl ester blends (1:4, w/w) was optimized when the active layer had a thickness of 70 nm. The photocurrents of the devices were enhanced as a result of the presence of the **PDI** moieties, thereby leading to improved power conversion efficiencies. © 2010 Wiley Periodicals, Inc. J Polym Sci Part A: Polym Chem 48: 1298–1309, 2010

KEYWORDS: conjugated polymers; copolymerization; heteroatom-containing polymers; perylene diimide; photovoltaic cells

INTRODUCTION Conjugated polymeric semiconductors possessing delocalized π-electron systems have potential applications such organic optoelectronic devices as light-emitting diodes (LEDs), organic field effect transistors (OFETs), and photovoltaic cells (PVCs). Many studies of polymer PVCs have focused on optimizing the configuration of the bulk heterojunctions, where the photoactive layers ordinarily consist of a conjugated polymer as an electron donor and a fullerene derivative as an electron acceptor.[1–5] Bulk heterojunctions based on regioregular poly(3-hexylthiophene)/[6,6]-phenyl-C_{61}-butyric acid methyl ester (P3HT/PCBM) composites as photoactive layers can display impressive power conversion efficiencies (PCEs) of up to 5%.[6–10] Furthermore, conjugated polymers featuring electron donor and acceptor (D–A) units in their main and/or side chains are quite attractive because of their tunable electronic properties, ambipolar charge transport abilities, and enlarged spectral absorption ranges.[11–19] The photovoltaic characteristics of D–A polymers are very susceptible to changes in the molecular structure. Accordingly, the selection of suitable donor and acceptor units for the polymer is an extremely critical task: their abilities to harvest light and generate, transfer, dissociate, and/or transport charge must all be taken into consideration. Previously, we have reported a new class of polymers, based on intramolecular D–A sidechain-tethered hexyl phenanthrenyl-imidazole polythiophene, that not only absorb light effectively but also exhibit enhanced charge transfer abilities—two desirable properties in photovoltaic applications—and, thus, good PCEs.[20–22]

Another class of promising PVCs materials-D–A double-cable polymers has been developed for a long period of time.[23–26] Because of the homogeneously distributed properties, they have featured a capacity to overcome the phase separation and have enabled the maximum interfacial interaction between donor and acceptor molecules. Consequently, a remarkable fluorescence quenching has been observed in these D–A double-cable polymers because of their fast and efficient intramolecular electron transfer from donor to acceptor.

Electron-deficient perylene-3,4,9,10-tetracarboxylic diimide (**PDI**) and its derivatives are attractive electron-withdrawing materials because of their excellent electron mobilities,[27–30] high electron affinities, large molar absorption coefficients, and good thermal and photochemical stabilities, enabling them to be applied to PVCs.[31–36] Another potential advantage of using a **PDI** moiety is that it undergoes inherent photoinduced charge transfer and energy transfer processes when covalently associated with an electron donor.[31,37–40] Therefore, we were inspired to incorporate **PDI** moieties as an electron-accepting components in the polymers described herein.

Poly(2,7-carbazole) derivatives are typical electron-donating materials that also exhibit good hole-transporting features.[41–44] Recently, a novel carbazole-containing polymer

Correspondence to: K.-H. Wei (E-mail: khwei@mail.nctu.edu.tw)

used as an electron donor in photovoltaic systems has manifested a very high PCE (approaching 6%).[45–47] Moreover, a new class of π-conjugated polymers comprising highly coplanar fused cyclopentadithiophene (**CPDT**) units in the polymer main chain has been developed.[48–52] Because its rigidly enforced planarity effectively extends the length of π-electron delocalization, the resulting reduced bandgap of the polymer and the increased strength of the intermolecular π–π interactions between polymer chains are beneficial to carrier transport. Several **CPDT**-containing polymers have displayed high hole mobilities[48,49] and have potential use in PVCs.[50–52] Therefore, the incorporation of carbazole and **CPDT** units as electron donors into polymer main chains is an attractive strategy for photovoltaic applications.

Based on the side chain-tethered D–A (double-cable) concept, we designed an extended conjugated polymer structure, which featured a backbone of highly coplanar **CPDT** units attached to hole-transporting carbazole segments; electron-withdrawing **PDI** moieties having a high absorption coefficient were incorporated as the side chain. We anticipated that the pendent **PDI** moieties would harvest photons more effectively in the visible region of the spectrum and result in substantial photoinduced electron transfer. In addition, these copolymers feature reasonable lowest unoccupied molecular orbital (LUMO) offsets (ca. 0.50 eV), which are sufficient to drive efficient charge dissociation after exciton formation.[53–55] In our molecular design, we introduced a long branched C_{24} alkyl group at the imide position of the **PDI** moiety and used a hexyl bridge to link the carbazole and **PDI** moieties to increase the solubility of the monomer **M1** and, thereby, promote its reactivity in polymerization. Moreover, we used **CPDT** monomers presenting long alkyl chains so that they would form alternating copolymers, thereby improving the solubility and broadening the spectral absorption range of the **PDI**-containing polymers. For comparison, we also prepared the corresponding copolymers lacking pendent **PDI** moieties. We synthesized these new copolymers using Suzuki coupling and analyzed them for their optical, electrochemical, and photovoltaic properties. Disappointingly, the efficiencies of devices incorporating these copolymers remained low, although they were enhanced when the electron-withdrawing **PDI** moieties were incorporated into the side chains.

EXPERIMENTAL

Materials

2,7-Dibromo-9*H*-carbazole (**1**),[56] 2-decyltetradecylamine (**5**),[57] 4,4-dioctyl-4*H*-cyclopenta[2,1-b:3,4-b′]dithiophene (**8**),[58] 4,4-bis(2-ethylhexyl)-4*H*-cyclopenta[2,1-b:3,4-b′]dithiophene (**9**),[50] and *N*-9′-heptadecanyl-2,7-dibromocarbazole (**M4**)[45] were prepared according to reported procedures. PCBM was purchased from Nano-C. All other reagents were used as received without further purification, unless stated otherwise.

Measurements and Characterization

^{1}H and ^{13}C NMR spectra were recorded using a Varian UNITY 300 MHz spectrometer. Mass spectra were obtained using a JEOL JMS-HX 110 spectrometer. Differential scanning calorimetry (DSC) was performed using a Perkin–Elmer Pyris 7 unit operated at heating and cooling rates of 10 and 40 °C min^{-1}, respectively; the glass transition temperatures (T_g) were determined from the second heating scan. Thermogravimetric analysis (TGA) was undertaken using a TA Instruments Q500; the thermal stabilities of the samples were determined under a N_2 atmosphere by measuring their weight losses while heating at a rate of 20 °C min^{-1}. Size exclusion chromatography (SEC) was performed using a Waters chromatography unit interfaced with a Waters 1515 differential refractometer; polystyrene was the standard and THF was the eluant. UV–vis and photoluminescence (PL) spectra of dilute chlorobenzene solutions (1×10^{-5} M) were measured using an HP 8453 diode-array spectrophotometer and a Hitachi F4500 luminescence spectrometer, respectively. Solid films for UV–vis and PL spectroscopic analyses were obtained by spin-coating chlorobenzene solutions of the copolymers (5 mg mL^{-1}) onto quartz substrates. Cyclic voltammetry (CV) was performed using a BAS 100 electrochemical analyzer operated at a scan rate of 50 mV s^{-1}; the solvent was anhydrous acetonitrile containing 0.1 M tetrabutylammonium hexafluorophosphate ($TBAPF_6$) as the supporting electrolyte. The potentials were measured against a Ag/Ag^+ (0.01 M $AgNO_3$) reference electrode; ferrocene/ferrocenium ion (Fc/Fc^+) was used as the internal standard. The onset potentials were determined from the intersection of two tangents drawn at the rising and background currents of the cyclic voltammogram. Topographic images of the copolymer/PCBM films (surface area: 5×5 μm^2) were obtained through atomic force microscopy (AFM) in the tapping mode under ambient conditions using a Digital Nanoscope IIIa instrument.

Fabrication and Characterization of Photovoltaic Devices

Indium tin oxide (ITO)–coated glass substrates were cleaned stepwise in detergent, water, acetone, and isopropyl alcohol (ultrasonication; 20 min each) and then dried in an oven for 1 h; subsequently, the substrates were treated with UV ozone for 10 min before use. A thin layer (ca. 30 nm) of poly(ethylene dioxythiophene):polystyrenesulfonate (PEDOT:PSS, Baytron P VP A1 4083) was spin coated at 5000 rpm onto the ITO substrates. After baking at 150 °C for 15 min in air, the substrates were transferred into a N_2-filled glovebox. The copolymers **P1**–**P4** were codissolved with PCBM in chlorobenzene (weight ratio: 1:2 or 1:4; total concentration: 20 mg mL^{-1}) and stirred continuously for 12 h at 50 °C. The photoactive layer was obtained by spin coating the blend solution onto the ITO/PEDOT:PSS surface at 1500 rpm for 60 s and then thermally annealing the system at 85 °C for 15 min before electrode deposition. The thicknesses of the photoactive layers were about 65–80 nm. Finally, an Al layer (100 nm) was thermally evaporated through a shadow mask under a vacuum of less than 1×10^{-6} torr. The effective layer area of one cell was 0.04 cm^2. The current density–voltage (*J*–*V*) characteristics were measured using a Keithley 236 source-meter. The photocurrent was measured under simulated AM 1.5 G irradiation at 100 mW cm^{-2} using a Xe lamp–based Newport 66902 150W solar simulator. The spectrum of the solar simulator was calibrated by a PV

measurement (PVM-154) monosilicon solar cell (NREL calibrated) to minimize spectral mismatch; a silicon photodiode (Hamamatsu S1133) was used to check the uniformity of the exposed area.

2,7-Dibromo-9-(6-bromohexyl)-9*H*-carbazole (2)

1,6-Dibromohexane (2.94 mL, 19.1 mmol) was added to a mixture of 2,7-dibromo-9*H*-carbazole (2.00 g, 6.15 mmol), KOH (0.41 g, 7.31 mmol), and *N,N*-dimethylformamide (DMF, 40 mL) at 0 °C. The system was stirred at room temperature for 24 h and then diluted with water (200 mL). The solution was extracted with EtOAc (3 × 50 mL), and the combined organic layers dried ($MgSO_4$) and concentrated under reduced pressure. The crude product was purified through column chromatography (EtOAc/hexane, 1:10) to afford **2** (2.25 g, 74.9%) as a white solid.

^{1}H NMR (300 MHz, $CDCl_3$): δ 1.27–1.53 (m, 4H), 1.79–1.92 (m, 4H), 3.39 (t, J = 6.6 Hz, 2H), 4.21 (t, J = 6.9 Hz, 2H), 7.34 (dd, J = 8.4, 1.2 Hz, 2H), 7.52 (d, J = 1.2 Hz, 2H), 7.89 (d, J = 8.1 Hz, 2H). ^{13}C NMR (75 MHz, $CDCl_3$): δ 26.3, 27.8, 28.6, 32.5, 33.6, 43.1, 111.9, 119.7, 121.3, 121.5, 122.6, 141.3. MS (m/z): $[M]^+$ calcd. for $C_{18}H_{18}Br_3N$, 486.9; found, 487.

2,7-Dibromo-9-(6-azidohexyl)-9*H*-carbazole (3)

Compound **2** (2.10 g, 4.30 mmol) and NaN_3 (1.41 g, 21.7 mmol) were dissolved in DMF (30 mL) and heated at 85 °C overnight. After cooling, the mixture was poured into water (200 mL) and extracted with EtOAc (3 × 50 mL). The combined organic layers were washed with brine, dried ($MgSO_4$), and concentrated under reduced pressure. The crude product was purified through column chromatography (EtOAc/hexane, 1:10) to afford **3** (1.75 g, 90.3%) as a viscous oil.

^{1}H NMR (300 MHz, $CDCl_3$): δ 1.39–1.60 (m, 6H), 1.81–1.90 (m, 2H), 3.25 (t, J = 6.9 Hz, 2H), 4.19 (t, J = 7.2 Hz, 2H), 7.34 (dd, J = 8.4, 1.2 Hz, 2H), 7.52 (d, J = 1.2 Hz, 2H), 7.89 (d, J = 8.1 Hz, 2H). ^{13}C NMR (75 MHz, $CDCl_3$): δ 26.4, 26.7, 28.6, 28.7, 43.0, 51.2, 111.8, 119.7, 121.2, 121.4, 122.5, 141.2. MS (m/z): $[M]^+$ calcd. for $C_{18}H_{18}Br_2N_4$, 450; found, 450.

2,7-Dibromo-9-(6-aminohexyl)-9*H*-carbazole (4)

A solution of **3** (1.5 g, 3.33 mmol) in Et_2O (20 mL) was added dropwise to a suspension of $LiAlH_4$ (0.18 g, 4.75 mmol) in Et_2O (20 mL) at 0 °C and then the system was stirred under N_2 for 2 h. The mixture was diluted with Et_2O and then saturated aqueous Na_2SO_4 was slowly added. After stirring for 1 h, the mixture was extracted with Et_2O (3 × 50 mL). The combined organic layers were washed with brine, dried ($MgSO_4$), and concentrated under reduced pressure. The crude product was purified through recrystallization (EtOH/hexane) to afford **4** (1.21 g, 85.6%) as a yellow solid.

^{1}H NMR (300 MHz, $CDCl_3$): δ 1.36–1.48 (m, 6H), 1.79–1.88 (m, 2H), 2.38 (s, 2H), 2.72 (t, J = 6.9 Hz, 2H), 4.17 (t, J = 7.2 Hz, 2H), 7.33 (dd, J = 8.4, 1.2 Hz, 2H), 7.51 (d, J = 1.2 Hz, 2H), 7.87 (d, J = 8.4 Hz, 2H). ^{13}C NMR (75 MHz, $CDCl_3$): δ 26.5, 26.9, 28.6, 33.6, 42.0, 43.1, 111.8, 119.6, 121.2, 121.4, 122.4, 141.2. MS (m/z): $[M]^+$ calcd. for $C_{18}H_{20}Br_2N_2$, 424; found, 424.

***N,N′*-Di(2-decyltetradecyl)perylene-3,4,9,10-tetracarboxylic Diimide (6)**

A mixture of perylene-3,4,9,10-tetracarboxylic acid anhydride (1.50 g, 3.82 mmol), $Zn(OAc)_2$ (0.84 g, 4.58 mmol), 2-decyltetradecylamine (4.07 g, 11.5 mmol), and quinoline (20 mL) was heated at 180 °C overnight under N_2. After cooling, the mixture was poured into MeOH (200 mL), treated with 2 M HCl (40 mL), and stirred overnight. The resulting precipitate was filtered off, washed sequentially with water and MeOH, and then dried under vacuum at 80 °C to afford **6** (3.55 g, 87.3%) as a red solid.

^{1}H NMR (300 MHz, $CDCl_3$): δ 0.81–0.87 (m, 12H), 1.20–1.33 (m, 80H), 1.99 (br, 2H), 4.11 (d, J = 6.9 Hz, 2H), 7.40 (d, J = 7.8 Hz, 4H), 8.53 (d, J = 7.8 Hz, 4H). ^{13}C NMR (75 MHz, $CDCl_3$): δ 14.1, 22.7, 26.5, 29.3, 29.6, 29.7, 30.1, 31.7, 31.9, 31.9, 36.7, 44.7, 122.6, 123.0, 125.7, 128.9, 130.8, 133.7, 163.2. MS (m/z): $[M]^+$ calcd. for $C_{72}H_{106}N_2O_4$, 1062.8; found, 1064.

***N*-(2-Decyltetradecyl)perylene-3,4,9,10-tetracarboxylic-3,4-anhydride-9,10-imide (7)**

A mixture of **6** (3.0 g, 2.82 mmol), KOH (0.43 g, 7.66 mmol), and *tert*-butyl alcohol (80 mL) was stirred at 85 °C for 40 min under N_2. Upon cooling, acetic acid (10 mL) and 2 M HCl (20 mL) were added. The red precipitate was filtered off and washed sequentially with water, MeOH, and cold acetone to afford **7** (1.34 g, 65.2%) as a red solid.

^{1}H NMR (300 MHz, $CDCl_3$): ^{1}H NMR (300 MHz, $CDCl_3$): δ 0.83–0.85 (m, 6H), 1.20–1.33 (m, 40H), 2.00 (m, 1H), 4.13 (m, 2H), 8.69 (br, 8H). MS (m/z): $[M]^+$ calcd. for $C_{48}H_{57}NO_5$, 727.4; found, 728.

***N*-(2-Decyltetradecyl)-*N′*-(2,7-dibromo-9-hexyl-9*H*-carbazole)perylene-3,4,9,10-tetracarboxylic Diimide (M1)**

A mixture of **4** (0.50 g, 1.18 mmol), **7** (0.78 g, 1.07 mmol), $Zn(OAc)_2$ (0.26 g, 1.42 mmol), and quinoline (15 mL) was heated at 180 °C for 4 h under N_2. After cooling, the mixture was poured into MeOH (100 mL), treated with 2 M HCl (20 mL), and stirred overnight. The resulting precipitate was collected by vacuum filtration, washed sequentially with water and MeOH, and then purified through column chromatography ($CHCl_2$) and recrystallization (EA/MeOH) to afford **M1** (0.75 g, 62%) as a dark red solid.

^{1}H NMR (300 MHz, $CDCl_3$): δ 0.78–0.87 (m, 6H), 1.14–1.47 (m, 44H), 1.75–1.82 (m, 4H), 1.98 (br, 1H), 4.07–4.15 (m, 6H), 7.21 (dd, J = 8.1 Hz, 1.5 Hz, 2H), 7.43 (d, J = 1.5 Hz, 2H), 7.73 (d, J = 8.1 Hz, 2H), 8.22 (dd, J = 8.4, 3.6 Hz, 4H), 8.41 (dd, J = 8.1, 3.3 Hz, 4H). ^{13}C NMR (75 MHz, $CDCl_3$): δ 14.1, 22.7, 26.5, 26.7, 26.8, 27.7, 28.6, 29.3, 29.6, 29.7, 30.1, 31.7, 31.9, 36.7, 40.3, 43.2, 44.7, 111.8, 119.6, 121.1, 121.3, 122.4, 122.6, 122.7, 122.9, 123.1, 125.8, 128.9, 128.9, 130.9, 133.8, 140.0, 141.1, 163.0, 163.4. MS (m/z): $[M]^+$ calcd. for $C_{66}H_{75}Br_2N_3O_4$, 1133.4; found, 1135. Anal. Calcd. for $C_{66}H_{75}Br_2N_3O_4$: C, 69.90; H, 6.67; N, 3.71. Found: C, 69.66; H, 6.62; N, 3.93.

2,6-Bis(4,4,5,5-tetramethyl-1,3,2-dioxaborolan-2-yl)-4,4-dioctyl-4*H*-cyclopenta[2,1-b:3,4-b′]dithiophene (M2)

n-BuLi (2.5 M, 5.40 mL, 13.5 mmol) was added dropwise to a stirred solution of **8** (1.80 g, 4.47 mmol) in anhydrous THF (20 mL) under N_2 at −78 °C. The mixture was stirred at this temperature for 1 h and then warmed to room temperature over 3 h. After cooling again to −78 °C, 2-isopropoxy-4,4,-5,5-tetramethyl[1,3,2]dioxaborolane (3.6 mL, 17.6 mmol) was added and then the mixture was warmed gradually to room temperature and stirred overnight. Water (100 mL) was added and the system extracted with Et_2O (3 × 50 mL). The combined organic layers were washed with brine (100 mL), dried ($MgSO_4$), and concentrated under reduced pressure. The crude product was washed with cold methanol and then recrystallized twice from ethanol to afford **M2** (1.98 g, 68%) as a yellow solid.

^{1}H NMR (300 MHz, $CDCl_3$): δ 0.80–0.90 (m, 10H), 1.10–1.28 (m, 20H), 1.34 (s, 24H), 1.75–1.80 (m, 4H), 7.40 (s, 2H). ^{13}C NMR (75 MHz, $CDCl_3$): δ 14.1, 22.6, 24.5, 24.8, 29.3, 30.0, 31.8, 37.8, 52.7, 84.0, 131.1, 143.9, 161.5. MS (*m*/*z*): $[M]^+$ calcd. for $C_{37}H_{60}B_2O_4S_2$, 654.4; found, 654. Anal. Calcd. for $C_{37}H_{60}B_2O_4S_2$: C, 67.89; H, 9.24. Found: C, 67.70; H, 9.42.

2,6-Dibromo-4,4-bis(2-ethylhexyl)-4*H*-cyclopenta[2,1-b:3,4-b′]dithiophene (M3)

A solution of **9** (1.25 g, 3.10 mmol) and *N*-bromosuccinimide (NBS, 1.10 g, 6.20 mmol) in DMF (20 mL) was stirred overnight under N_2 at room temperature. The resulting solution was poured into water (200 mL) and extracted with $CHCl_2$ (3 × 50 mL). The combined organic layers were washed with brine, dried ($MgSO_4$), and concentrated under reduced pressure. The crude product was purified through column chromatography (hexane) to afford **M3** (1.43 g, 82.2%) as a pale yellow oil.

^{1}H NMR (300 MHz, $CDCl_3$): δ 0.57–0.64 (m, 6H), 0.76–0.81 (m, 6H), 0.88–1.05 (m, 18H), 1.74–1.86 (m, 4H), 6.93 (dt, J = 2.7, 0.9 Hz, 2H). ^{13}C NMR (75 MHz, $CDCl_3$): δ 10.6, 14.0, 22.7, 27.3, 28.5, 32.0, 35.1, 43.0, 54.9, 110.7, 125.2, 136.6, 155.5. MS (*m*/*z*): $[M]^+$ calcd. for $C_{25}H_{36}Br_2S_2$, 560.1; found, 560. Anal. Calcd. for $C_{25}H_{36}Br_2S_2$: C, 53.57; H, 6.47. Found: C, 53.99; H, 6.56.

General Procedure for Synthesizing the Alternating Copolymers P1–P4

Aqueous K_2CO_3 (2M, 1.6 mL) and Aliquat 336 (ca. 20 mg) were added to a mixture of **M1** (100 mg, 88.1 μmol), **M2** (115.4 mg, 176.2 μmol), and **M3** (49.4 mg, 88.1 μmol) in toluene (3.2 mL). After degassing, tetrakis(triphenylphosphine)-palladium (5 mol %) was added under N_2. The reaction mixture was heated at 100 °C for 36 h and then benzeneboronic acid (42.9 mg, 0.35 mmol) and bromobenzene (55.3 mg, 0.35 mmol), the end-capping units, were added individually to the solution, which was then heated under reflux for 6 h each time. The reaction mixture was cooled to room temperature and the product precipitated in a mixture of methanol and water (8:2, v/v; 100 mL). The crude polymer was collected, dissolved in THF, and reprecipitated in methanol. Finally, the polymer was washed with acetone for 72 h in a Soxhlet apparatus and then dried under vacuum to give **P1** (119.0 mg, 62%).

^{1}H NMR (300 MHz, $CDCl_3$): δ 0.69–0.85 (m, 38H), 1.05–1.20 (m, 102H), 1.61–1.90 (m, 17H), 4.01–4.33 (m, 6H), 7.03 (br, 6H), 7.30–7.76 (m, 6H), 7.98–8.58 (m, 8H). ^{13}C NMR (75 MHz, $CDCl_3$): δ 10.7, 14.1, 22.6, 22.7, 22.9, 24.6, 26.5, 27.5, 28.6, 29.2, 29.3, 29.6, 29.7, 30.1, 31.8, 31.9, 34.1, 35.3, 36.6, 37.8, 40.3, 43.1, 44.7, 54.2, 104.8, 117.2, 117.8, 120.5, 121.9, 122.9, 123.1, 125.5, 126.1, 128.4, 128.5, 129.1, 130.7, 131.2, 131.9, 132.1, 132.2, 133.5, 134.3, 138.2, 138.5, 141.5, 145.7, 158.2, 158.5, 158.8, 162.9, 163.2, 163.6. Anal. Calcd.: C, 77.74; H, 8.56; N, 1.93. Found: C, 75.48; H, 8.23; N, 1.79.

P2

Using an identical polymerization procedure as that described earlier for **P1**, a mixture of **M1** (49.0 mg, 43.2 μmol), **M2** (42.4 mg, 64.8 μmol), and **M3** (12.1 mg, 21.6 μmol) in toluene (1.4 mL) was copolymerized to give **P2** (40.1 mg, 53%).

^{1}H NMR (300 MHz, $CDCl_3$): δ 0.69–0.85 (m, 56H), 1.20 (br, 164H), 1.61–1.89 (m, 26H), 4.01–4.34 (m, 12H), 7.03 (br, 8H), 7.31–7.75 (m, 12H), 7.96–8.61 (m, 16H). Anal. Calcd.: C, 78.42; H, 8.40; N, 2.37. Found: C, 75.94; H, 8.02; N, 2.14.

P3

Using an identical polymerization procedure as that described earlier for **P1**, a mixture of **M2** (52.1 mg, 79.6 μmol), **M3** (22.3 mg, 39.8 μmol), and **M4** (22.4 mg, 39.8 μmol) in toluene (1.3 mL) was copolymerized to give **P3** (41.5 mg, 65%).

^{1}H NMR (300 MHz, $CDCl_3$): δ 0.69–0.85 (m, 30H), 1.06–1.20 (m, 88H), 1.58–1.91 (m, 16H), 2.39 (br, 2H), 4.64 (br, 1H), 7.03 (br, 6H), 7.54–7.61 (m, 4H), 8.05 (br, 2H). Anal. Calcd.: C, 77.70; H, 9.47; N, 0.87. Found: C, 75.36; H, 8.55; N, 0.87.

P4

Using an identical polymerization procedure as that described earlier for **P1**, a mixture of **M2** (119.5 mg, 182.5 μmol) and **M3** (102.3 mg, 182.5 μmol) in toluene (2.6 mL) was copolymerized to give **P3** (108.2 mg, 74%).

^{1}H NMR (300 MHz, $CDCl_3$): δ 0.67–0.87 (m, 18H), 1.05–1.20 (m, 42H), 1.58–1.88 (m, 8H), 7.01 (d, J = 9 Hz, 4H). ^{13}C NMR (75 MHz, $CDCl_3$): δ 10.8, 14.2, 22.7, 23.0, 24.7, 27.6, 28.7, 29.3, 29.4, 30.2, 31.9, 34.2, 35.4, 37.8, 43.2, 54.0, 54.1, 117.0, 117.7, 134.7, 135.1, 137.9, 138.4, 158.0, 158.4. Anal. Calcd.: C, 74.75; H, 9.28. Found: C, 71.92; H, 8.82.

RESULTS AND DISCUSSION

Synthesis and Characterization of the Copolymers

Schemes 1 and 2 outline our synthetic routes toward the monomers and copolymers. *N*-Alkylation of 2,7-dibromo-9*H*-carbazole (**1**) with excess 1,6-dibromohexane and KOH gave compound **2**, which we subjected to azidation to afford the azide **3**, which was then transformed into the primary amine **4** through hydride reduction. Condensation of perylene-3,4,9,10-tetracarboxylic acid anhydride with 2-decyltetradecylamine using zinc acetate as catalyst gave a good yield of

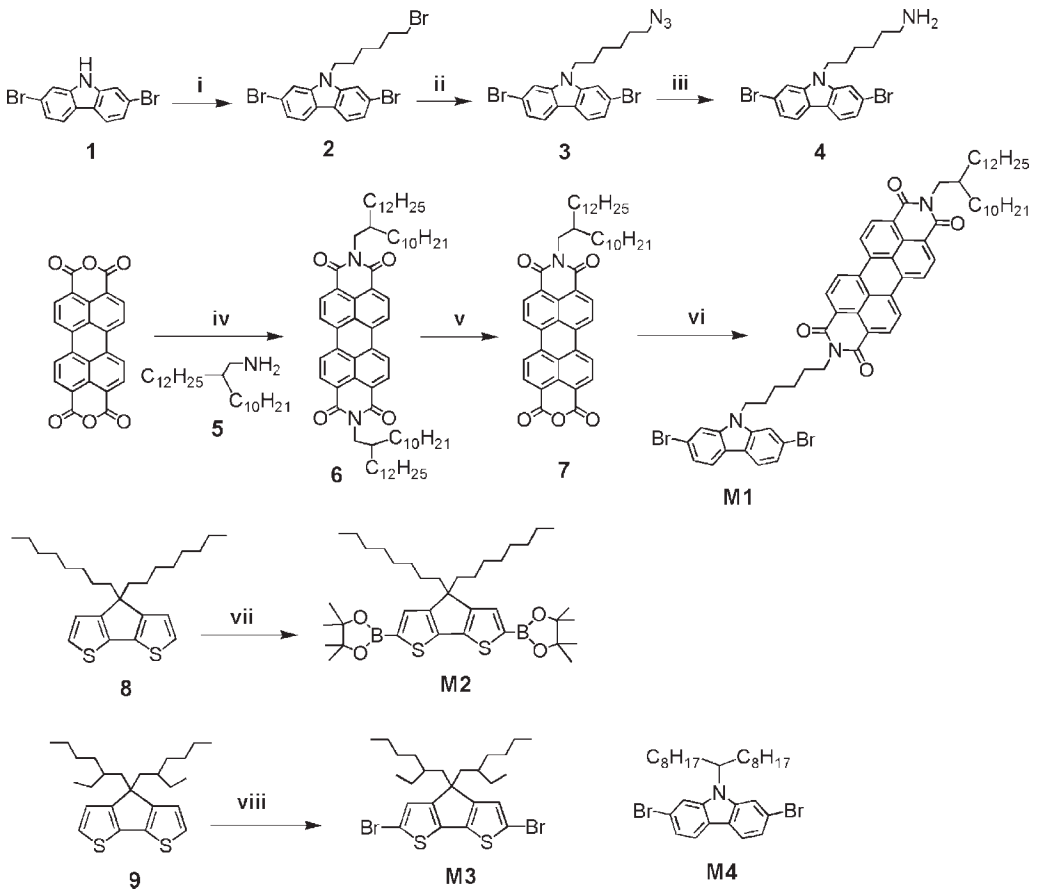

SCHEME 1 Synthetic routes of the monomers. Reagents: (i) 1,6-dibromohexane, KOH, DMF; (ii) NaN_3, DMF; (iii) $LiAlH_4$, Et_2O; (iv) 2-decyl-tetradecylamine, $Zn(OAc)_2$, quinoline; (v) *t*-BuOH, KOH; (vi) **4**, $Zn(OAc)_2$, quinoline; (vii) THF, *n*-BuLi, 2-isopropoxy-4,4,5,5-tetramethyl-[1,3,2]dioxaborolane; and (viii) NBS, DMF.

the symmetric perylene tetracarboxylic diimide **5**, which was then semihydrolyzed to generate the monoimide monoanhydride **6**; subsequent condensation with **4** afforded the monomer **M1**. NBS-mediated dibromination of dioctylcyclopentadithiophene (**8**) afforded the monomer **M2**; the boronated monomer **M3** was prepared through dilithiation of compound **9** with *n*-BuLi, followed by quenching with 2-isopropoxy-4,4,5,5-tetramethyl[1,3,2]dioxaborolane. As indicated in Scheme 2, the alternating copolymers **P1**–**P4** were obtained through Suzuki polycondensations using various monomer **M1**–**M4** mixtures. From the ratio of the integrations of the peaks of NMR aliphatic protons (—N—CH_2— for **P1**–**P2** at 4.01–4.34 ppm and —N—CH— for **P3** at 4.64 ppm) to that of aromatic protons (thiophene-H at 7.03 ppm), we estimated the output compositions of monomers **M1**–**M4** present in the copolymers **P1**–**P3**. The final compositions of the synthesized polymers were very close to the feed ratios, and the output ratios of **P1**–**P3** are summarized in Table 1. **P1** and **P2**, featured solubilizing **PDI** moieties in their polymer side chains, had weight-average molecular weights (M_w), determined through gel permeation chromatography (GPC) using polystyrene as standards, of 21.1 and 11.1 kg mol^{-1}, respectively, and polydispersities of 1.65 and 1.60, respectively. The lower molecular weight of **P2** was due to the twofold feed ratio of monomer **M1**, which had relatively poor solubility during the polymerization reaction. For control experiments, we synthesized the copolymer **P3** (M_w: 19.3 kg mol^{-1}; polydispersity: 1.43) through conjugation of the carbazole segment with **CPDT** in the polymer backbone. Moreover, we also prepared the **CPDT**-only polymer **P4** (M_w: 30.8 kg mol^{-1}; polydispersity: 1.65). The copolymers **P1**–**P4** are generally soluble in common organic solvents, including toluene, THF, $CHCl_3$, and chlorobenzene, with **P4** exhibiting the best solubility among the four. The synthesized monomers and copolymers were characterized using ^1H and ^{13}C NMR spectroscopy and mass spectrometry. As revealed in Figure 1, all of the copolymers exhibited outstanding thermal stabilities, with 5% weight losses temperatures (T_d) greater than 400 °C under N_2 atmosphere. We investigated the thermal behavior of these copolymers through DSC analysis, which revealed no obvious thermal transitions for **P1**–**P3** within the temperature range from 40 °C to 320 °C, except for **P4**, which exhibited a distinct glass transition temperature (T_g) at 184 °C; thus, **P1**–**P4** display amorphous properties, with the incorporation of relatively stiff carbazole segments and bulky pendent **PDI** moieties probably restraining the

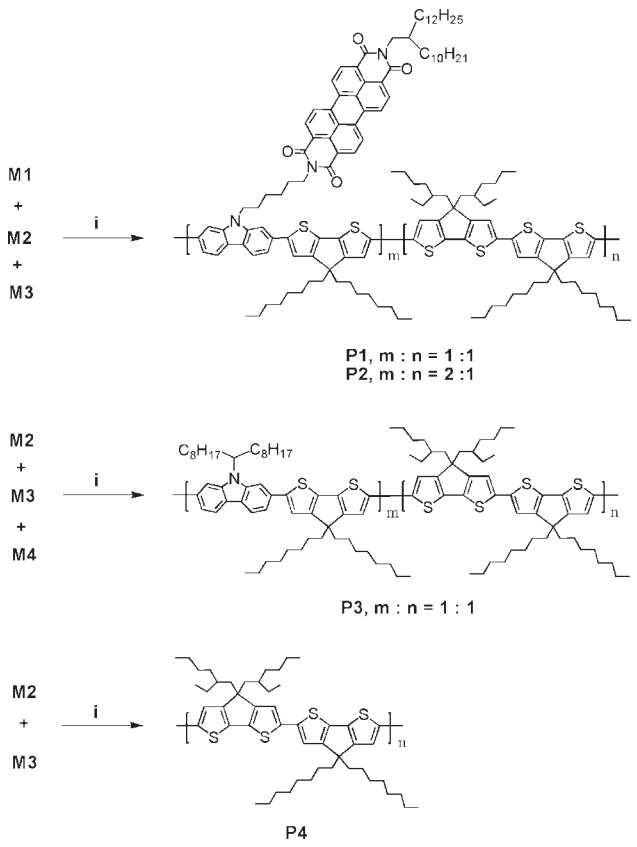

SCHEME 2 Synthetic routes of the copolymers. Reagents: (i) 2M K_2CO_3 (aq)/toluene, aliquat 336, $Pd(PPh_3)_4$.

movement of the polymer chains. Table 1 summarizes the yields, molecular weights, polydispersities, and thermal properties of the copolymers.

Photophysical Properties

Figure 2 displays absorption spectra of the monomer **M1** and the copolymers **P1**–**P4**, recorded from dilute (1×10^{-5} M) chlorobenzene solutions and solid films; Table 2 summarizes the spectral data. The broad absorption bands of **P1**–**P3** in solution in the range 300–700 nm originated from the copolymer backbones, that is, the extremely coplanar **CPDT**-based units and the conjugated carbazole–**CPDT** segments. The spectrum of **P3** featured a maximum absorption wavelength at 556 nm; **P1** and **P2** exhibited two distinct absorption peaks at 491–494 and 527–530 nm as a result of π–π^* transitions in the pendent **PDI** moieties of the monomer **M1**, which displays major absorptions at 490 and 526 nm, consistent with previous reports.[37–39] The maximum absorption wavelength of **P4** was 586 nm, comparable with that of the related homopolymer **PCPDT**.[59–61] **P1**–**P3** displayed hypsochromic shifts of about 30–59 nm, relative to **P4**, of the corresponding maximum wavelength absorption, presumably because of the carbazole–**CPDT** units presenting relatively shorter conjugated length. The broader absorptions of **P1** and **P2**, relative to that of monomer **M1**, implied that they featured extended conjugation lengths as a result of linking the coplanar **CPDT**-based units with the monomer **M1** units in the polymer backbones. The absorption spectra of **P1**–**P4** in the solid state were similar to their corresponding solution spectra, indicating that these copolymers did not self-assemble or aggregate in their solid films, consistent with the characteristics of **CPDT**-based polymers reported in the literature.[61]

The optical band gaps (E_g^{opt}) of **P1**–**P4**, estimated from the onsets of absorption in their solid films, were in the range of 1.82–1.88 eV. As expected, the optical band gaps of **P1**–**P3** were slightly higher than that of **P4**, due to the decreasing content of **CPDT**-based units. Generally, the amount of absorbed light depends not only on the absorption wavelength but also on the intensity of the absorption; hence, we estimated the molar absorption coefficients (ε), calculated using Beer's law, of these copolymers at the same concentrations in chlorobenzene. As indicated in Figure 2, **P3** displays a relatively low absorption coefficient (3.2×10^4 at $\lambda_{max} =$ 556 nm) relative to those of **P1** (4.9×10^4 at $\lambda_{max} = 530$ nm), **P2** (5.5×10^4 at $\lambda_{max} = 527$ nm), and **P4** (5.3×10^4 at $\lambda_{max} = 584$ nm). We suspect that the molar absorption coefficients of **P1** and **P2** are larger than that of **P3** because of the large degrees of light absorption by the pendent **PDI** moieties of the monomer **M1** (6.3×10^4 at $\lambda_{max} = 526$ nm), thereby facilitating greater photon harvesting. Figure 3 displays the PL spectra of the copolymers in dilute (1×10^{-5} M) chlorobenzene and as solid films, recorded with an excitation wavelength of 460 nm. In solution, the PL of **P3** increased relative to that of **P4,** probably as a result of the introduction of the highly fluorescent carbazole segments in the polymer backbone; in contrast, the PL of the **PDI**-containing copolymers **P1** and **P2** was quenched dramatically relative to that of **P3**, even though we positioned hexyl bridges between the pendent **PDI** moieties and the polymer backbone. In the solid films, we observed only slight PL for **P1**–**P4** at wavelengths in the range 600–800 nm, although the PL quenching of **P1** was more apparent than that of **P3**. The presence of PL quenching of the D–A bridge polymers in both solution and solid film suggests that photoinduced

TABLE 1 Polymerization Results and Thermal Properties of the Copolymers

Polymer	Feed Ratio (*m*:*n*)	Output Ratio[a] (*m*:*n*)	Yield (%)	M_n (10^3)	M_w (10^3)	PDI	DSC (T_g)	TGA (T_d)
P1	1:1	0.98:1	62	12.8	21.1	1.65	n.d.	416
P2	2:1	1.95:1	53	7.1	11.1	1.60	n.d.	418
P3	1:1	1.04:1	65	13.5	19.3	1.43	n.d.	411
P4	0:*n*	0:*n*	74	18.7	30.8	1.65	184	404

[a] Output ratios (*m*:*n*) of the copolymers were estimated from the integrations of the proton NMR spectra.

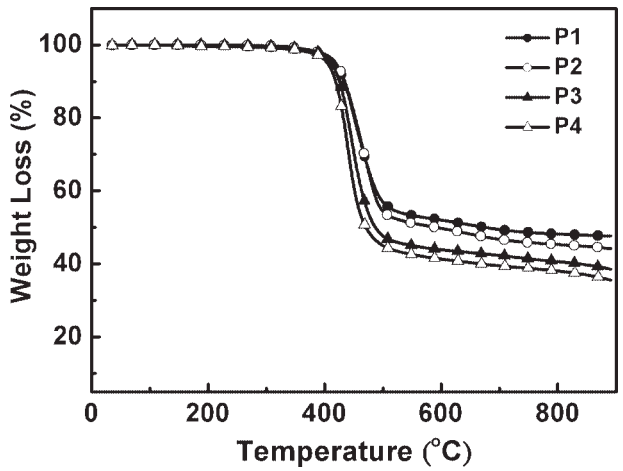

FIGURE 1 TGA thermograms of the copolymers recorded at a heating rate of 20 °C min^{-1} under a N_2 atmosphere.

electron transfer—through the polymer donors to the pendent **PDI** moieties in the excited state—was more efficient in polymer **P1** than others.[24,62,63]

Electrochemical Properties

We used CV to investigate the redox behavior of the copolymers and, thereby, estimate their highest occupied molecular orbital (HOMO) and LUMO energy levels. Figure 4 displays the electrochemical behavior of the copolymers in solid films; Table 2 summarizes the relevant data. The carbazole-containing copolymers **P1**–**P3** exhibited reversible oxidations; their onset potentials (ca. 0.14–0.18 V) were slightly larger than that of **P4** (0.12 V) because **P1**–**P3** contain less easily oxidizable carbazole segments in their polymer backbones. The CV traces of **P3** and **P4** feature irreversible reductions; we assign the onset potentials, very close at 2.31 and 2.32 V, for reduction of the **CPDT** units. In contrast, **P1** and **P2** underwent partially reversible reductions with onset potentials of 1.13 and 1.10 V, which we attribute for reduction of the **PDI** moieties, consistent with the value (1.19 V) reported previously.[32] On the basis of the onset potentials, we estimated HOMO energy levels of **P1**–**P4** to be 4.94, 4.94, 4.98, and 4.92 eV, respectively, with LUMO energy levels of 3.67, 3.70, 2.48, and 2.49 eV, respectively, according to the energy level of the ferrocene reference (4.8 eV below vacuum level).[64] Thus, copolymers **P1** and **P2** featured lower LUMO energy levels relative to that of **P3**, implying that the

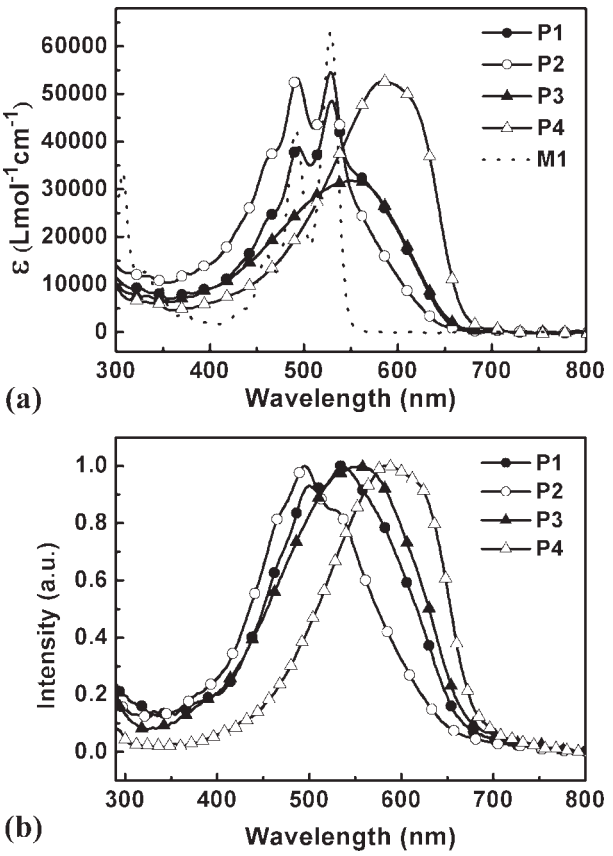

FIGURE 2 UV–vis absorption spectra of the copolymers **P1**–**P4** (a) in dilute chlorobenzene solutions (1×10^{-5} M) and (b) as solid films.

incorporation of electron-withdrawing pendent **PDI** moieties into the polymer side chains effectively lowered the LUMO energy levels. The resulting LUMO offsets (LUMO of PCBM is ca. 4.2 eV)[55] were 0.53 and 0.50 eV, respectively; these values are greater than the lowest value (0.3 eV)[53–55] required to drive efficient charge dissociation.

Photovoltaic Properties

The photovoltaic properties of the copolymers pristine **P1** and **P2** were studied by adjusting their concentrations. When both **P1** and **P2** were spin coated using the concentration of 15 mg mL^{-1} in chlorobenzene, the thickness of **P1** and **P2** films after drying was about 65 and 60 nm, respectively. **P1** and **P2** exhibited the value of V_{oc} of 0.41 and 0.45

TABLE 2 Optical and Redox Properties of the Copolymers

	Absorption, λ_{max} (nm)							
	Solution	Film	ε (10^4)[a]	E_g^{opt} (eV)[b]	E_{onset}^{ox} (V)	E_{onset}^{red} (V)	HOMO (eV)[c]	LUMO (eV)[c]
P1	494, 530	500, 536	4.9	1.85	0.14	1.13	4.94	3.67
P2	491, 527	495, 527	5.5	1.88	0.14	1.10	4.94	3.70
P3	556	556	3.2	1.83	0.18	2.32	4.98	2.48
P4	586	584	5.3	1.82	0.12	2.31	4.92	2.49

[a] Absorption coefficients were determined at λ_{max} for chlorobenzene solutions (1×10^{-5} M).

[b] Estimated from the onset wavelength absorptions of the solid films.

[c] Calculated from the corresponding onset potentials.

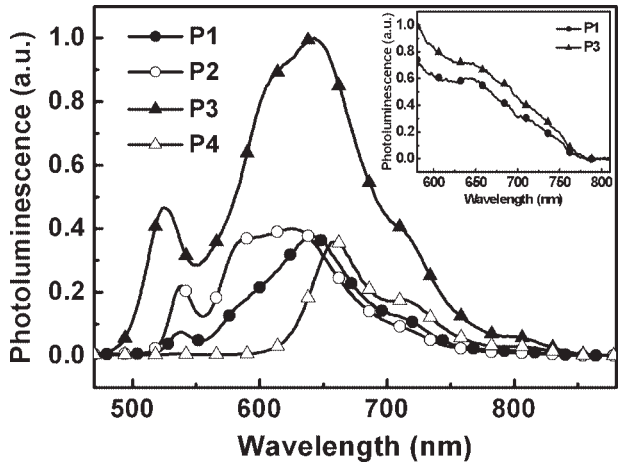

FIGURE 3 PL spectra of the copolymers in dilute chlorobenzene solutions (1×10^{-5} M). Inset: PL spectra of copolymers **P1** and **P3** as solid films. The PL intensity was normalized after dividing by the corresponding absorbance. All PL spectra, for solutions and films, were recorded with excitation at 460 nm.

V, J_{sc} of 0.113 and 0.099 mA cm^{-2}, fill factor (FF) of 0.267 and 0.255, and PCE of 0.012 and 0.011%, respectively. When the thicknesses of **P1** and **P2** were increased to about 88 and 80 nm, respectively, (coated with 20 mg mL^{-1}), the efficiencies of them did not significantly improve, with PCE of 0.011% for **P1** and 0.010% for **P2**.

Furthermore, we investigated the photovoltaic properties of the copolymers in bulk heterojunction solar cells having the sandwich structure ITO/PEDOT:PSS/copolymer:PCBM (1:2 or 1:4, w/w)/Al. The photoactive layers were spin coated from chlorobenzene solutions. Because the performance of PVCs is strongly dependent on the D–A ratio and the thickness of the active layer,[13,46,52] we constructed a series of devices featuring active layers possessing a variety of polymer-to-PCBM ratios and thicknesses. Figure 5 presents *J–V* curves of the PVCs incorporating 1:2 and 1:4 (w/w) blends of the copolymers and PCBM; Table 3 summarizes their characteristics.

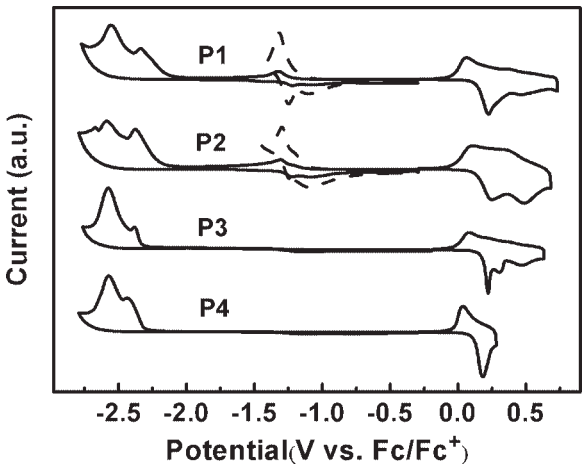

FIGURE 4 Cyclic voltammograms of the copolymers as solid films.

The devices based on **P1–P3**:PCBM exhibited similar open circuit voltages (V_{oc}) of 0.50–0.56 V and the **P4**:PCBM-based device featured a value of V_{oc} of 0.40–0.42 V; these values are related to the difference between the HOMO energy level of the copolymers and the LUMO energy level of PCBM.[54] Devices prepared from **P1–P3** exhibited larger values of V_{oc} relative to that prepared from **P4** because the former possess slightly lower lying HOMO energy levels, presumably because of the carbazole segments in their polymer backbones. The short-circuit current densities (J_{sc}) of the devices incorporating the **P1** and **P2** blends were significantly improved relative to those containing the **P3** and **P4** blends, presumably because of the effect of the pendent **PDI** moieties, with their enhanced photon harvesting, efficient photoinduced charge transfer/charge dissociation, and electron-transporting ability. Notably, the value of J_{sc} decreased upon increasing the content of **PDI** moieties in the polymer, regardless of the blend ratio (1:2 or 1:4), presumably because of the lower molecular weight, with a relatively shorter polymer backbone, which perhaps diminished the degree of charge transport among the polymer chains.[46,65,66] The **P2** blend exhibited a value of J_{sc} of 0.855 mA cm^{-2}, V_{oc} of 0.56 V, a FF of 0.359, and a PCE of 0.172% at the 1:2 blend ratio; the **P1** blend displayed superior performance,

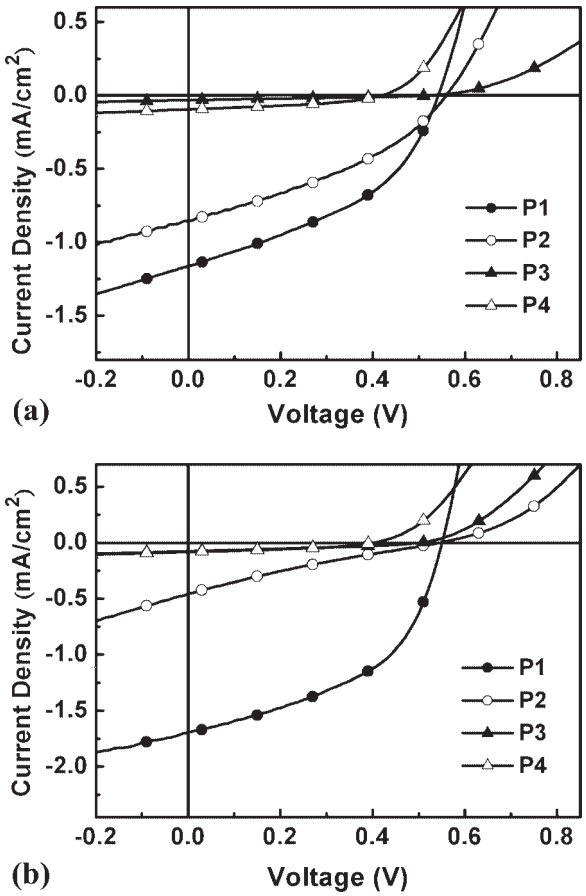

FIGURE 5 *J–V* characteristics of polymer PVCs incorporating **P1–P4**:PCBM films prepared at blend ratios (w/w) of (a) 1:2 and (b) 1:4.

TABLE 3 Photovoltaic Properties of Polymer Solar Cells Incorporating **P1**–**P4**:PCBM Blends Prepared at 1:2 and 1:4 Weight Ratios

Polymer:PCBM (w/w)		Thickness (nm)[a]	J_{sc} (mA cm^{-2})	V_{oc} (V)	FF	PCE (%)
P1	1:2	72	1.159	0.54	0.427	0.267
	1:4	70	1.703	0.55	0.485	0.454
P2	1:2	68	0.855	0.56	0.359	0.172
	1:4	65	0.457	0.55	0.212	0.053
P3	1:2	83	0.032	0.53	0.312	0.005
	1:4	78	0.076	0.50	0.334	0.013
P4	1:2	77	0.096	0.42	0.396	0.016
	1:4	72	0.083	0.40	0.396	0.013

[a] The thickness of the active layer was measured from AFM.

with values of J_{sc} of 1.159 mA cm^{-2}, V_{oc} of 0.54 V, FF of 0.427, and PCE of 0.267% under the same fabrication conditions. The device performance of **P1** blend improved upon increasing the amount of PCBM. Similar phenomena have been observed in studies of other amorphous polymer:PCBM systems.[1,2,13,47] For the 1:4 blends, **P1** again exhibited the better performance, with values of J_{sc} of 1.703 mA cm^{-2}, V_{oc} of 0.55 V, FF of 0.485, and PCE of 0.454%.

Figure 6 displays the surface morphologies determined from AFM measurements. Samples of the **P1**–**P4**:PCBM (1:4 w/w) blended films were spin coated from their corresponding chlorobenzene solutions, identical to the procedure used to fabricate the active layers of the devices. We observe coarse phase separation in the images of these polymer blends. The morphology of the **P2** blend is somewhat different from those of the others, presumably because of its low molecular weight and relatively poor solubility.[14] The **P1**–**P3** blends feature larger domains than those of the **P4** blend, particularly that for **P1**, which displays island-like domains. The root-mean-square roughness of the **P1**–**P3** blends was 4.15, 3.91, and 5.82 nm, respectively, significantly greater than that of **P4** (1.84 nm). The greater phase segregation and rougher surfaces of the **P1**–**P3** blend films presumably arose because of their poor miscibility with PCBM[15,16]—a result of their relatively poor solubility and low molecular weight after introducing the bulky carbazole segments and pendent **PDI** moieties. Even though the blends of **P1** and **P2** revealed these imperfections, which may have hampered their charge

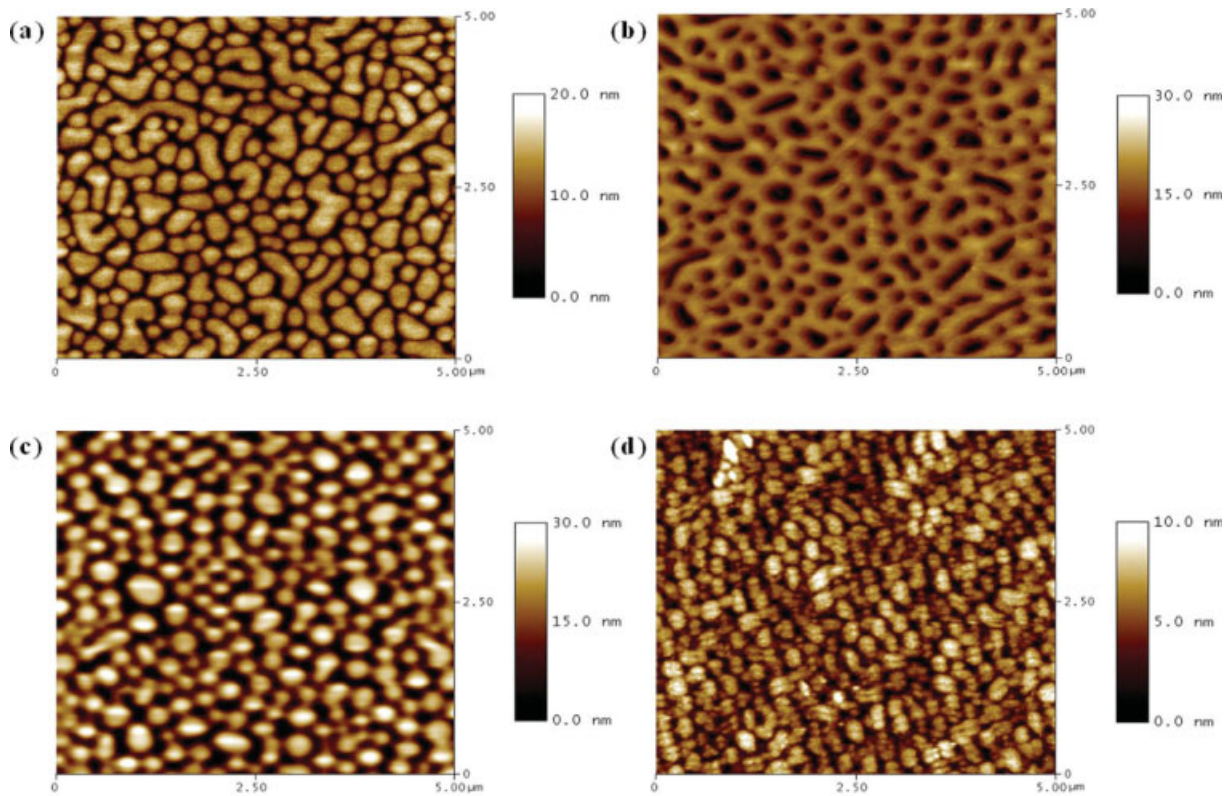

FIGURE 6 Topographic AFM images of the copolymer:PCBM (1:4, w/w) blends incorporating (a) **P1**, (b) **P2**, (c) **P3**, and (d) **P4**.

dissociation and transport properties, the performances of the devices based on the **PDI**-containing polymers were better than that of the **P4**-containg device, that is, the advantages bestowed by the pendent **PDI** moieties effectively compensated for these disadvantages. Although the selection of these donors and acceptor was probably a promising approach to photovoltaic application, the efficiencies of the designed **PDI**-containing polymers remained moderate. From the AFM images, we assume that the coarse phase separation behavior of the **PDI** moieties may have significant influence on the device performance. The strong electron-withdrawing **PDI** moieties would probably compete with PCBM when accepting the photogenerated electrons. Furthermore, the electrons would be easily trapped by the large/scattered **PDI** moieties, thereby leading to inefficient electron transport to the electrode, and thus low device efficiencies.

Next, we examined the effect that the thickness of the **P1**:PCBM blend had on the device performance. Figure 7 displays the *J–V* characteristics; Table 4 summarizes the associated data. We varied the thickness of the active layer in the range 60–112 nm by adjusting the concentrations (15–35 mg mL^{-1}) of the blended solutions coated at the same spin rate. The optimized thickness of the active layer was presented at 70 nm. When we reduced the thickness to 60 nm or increased it to 112 nm, we did not obtain higher PCEs because of concomitant decreases in both J_{sc} and FF. The thicker active layer (112 nm) resulted in significantly reduced value of J_{sc} (0.789 mA cm^{-2}), possibly because of the unfavorable influence of impeded charge transport or charge recombination.[67,68] In contrast, we attribute the decreased value of J_{sc} (1.431 mA cm^{-2}) of the device featuring the thinner active layer to its diminished absorbance of irradiated light.

CONCLUSIONS

We have prepared a series of new cyclopentadithiophene-based copolymers through conjugation with transporting carbazole segments in the polymer backbones and incorporation of electron-deficient **PDI** moieties into the side chains. The larger molar absorption coefficients and more efficient photoinduced electron transfer of these copolymers resulted from the presence of the pendent **PDI** moieties. Moreover, the **PDI**-containing copolymers exhibited reasonable and sufficient LUMO offsets to allow efficient charge dissociation. As a result, the photocurrents of the devices were enhanced after incorporation of the **PDI** moieties; the optimized PCE occurred when using a 1:4 (w/w) copolymer:PCBM blend having a thickness of 70 nm.

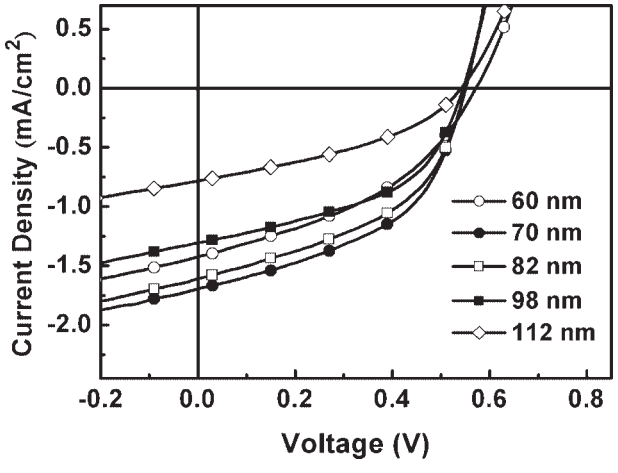

FIGURE 7 *J–V* characteristics of polymer PVCs incorporating **P1**:PCBM (1:4, w/w) blends of various thicknesses.

TABLE 4 Photovoltaic Properties of Polymer Solar Cells Incorporating **P1**:PCBM (1:4, w/w) Blend Layers of Various Thicknesses

Concentration of Blend Solution (mg mL^{-1})	Thickness (nm)[a]	J_{sc} (mA cm^{-2})	V_{oc} (V)	FF	PCE (%)
15	60	1.431	0.56	0.406	0.325
20	70	1.703	0.55	0.485	0.454
25	82	1.614	0.55	0.466	0.414
30	98	1.311	0.55	0.481	0.347
35	112	0.789	0.54	0.387	0.165

[a] The thickness of the active layer was controlled by varying the concentration of the spin-coated blend solution; the spin rate was fixed at 1500 rpm.

The authors thank the National Science Council for financial support through project NSC 98-2120-M-009-006.

REFERENCES AND NOTES

1 Wienk, M. M.; Kroon, J. M.; Verhees, W. J. H.; Knol, J.; Hummelen, J. C.; van Hal, P. A.; Janssen, R. A. J Angew Chem Int Ed 2003, 42, 3371–3375.

2 Hoppe, H.; Niggemann, M.; Winder, C.; Kraut, J.; Hiesgen, R.; Hinsch, A.; Meissner, D.; Sariciftci, N. S. Adv Funct Mater 2004, 14, 1005–1011.

3 Egbe, D. A. M.; Nguyen, L. H.; Schmidtke, K.; Wild, A.; Sieber, C.; Guenes, S.; Sariciftci, N. S. J Polym Sci Part A: Polym Chem 2007, 45, 1619–1631.

4 Schulz, G. L.; Chen, X.; Holdcroft, S. Appl Phys Lett 2009, 94, 023302.

5 Tang, W. H.; Kietzke, T.; Vemulamada, P.; Chen, Z.-K. J Polym Sci Part A: Polym Chem 2007, 45, 5266–5276.

6 Ma, W.; Yang, C.; Gong, X.; Lee, K.; Heeger, A. J. Adv Funct Mater 2005, 15, 1617–1622.

7 Li, G.; Shrotriya, V.; Huang, J.; Yao, Y.; Moriarty, T.; Emery, K.; Yang, Y. Nat Mater 2005, 4, 864–868.

8 Reyes-Reyes, M.; Kim, K.; Carroll, D. L. Appl Phys Lett 2005, 87, 083506.

9 Kim, Y.; Cook, S.; Tuladhar, S. M.; Choulis, S. A.; Nelson, J.; Durrant, J. R.; Bradley, D. D. C.; Giles, M.; McCulloch, I.; Ha, C.-S.; Ree, M. Nat Mater 2006, 5, 197–203.

10 Chiu, M.-Y.; Jeng, U.-S.; Su, C.-H.; Liang, K. S.; Wei, K.-H. Adv Mater 2008, 20, 2573–2578.

11 Huo, L. J.; Tan, Z.; Wang, X.; Zhou, Y.; Han, M. F.; Li, Y. F. J Polym Sci Part A: Polym Chem 2008, 46, 4038–4049.

12 Xin, H.; Guo, X.; Kim, F. S.; Ren, G.; Watson, M. D.; Jenekhe, S. A. J Mater Chem 2009, 19, 5303–5310.

13 Gadisa, A.; Mammo, W.; Andersson, L. M.; Admassie, S.; Zhang, F. L.; Andersson, M. R.; Inganäs, O. Adv Funct Mater 2007, 17, 3836–3842.

14 Lindgren, L. J.; Zhang, F. L.; Andersson, M.; Barrau, S.; Hellström, S.; Mammo, W.; Perzon, E.; Inganäs, O.; Andersson, M. R. Chem Mater 2009, 21, 3491–3502.

15 Liang, Y.; Feng, D.; Wu, Y.; Tsai, S.-T.; Li, G.; Ray, C.; Yu, L. J Am Chem Soc 2009, 131, 7792–7799.

16 Lai, M.-H.; Chueh, C.-C.; Chen, W.-C.; Wu, J.-L.; Chen, F.-C. J Polym Sci Part A: Polym Chem 2009, 47, 973–985.

17 Zhou, E.; Yamakawa, S.; Tajima, K.; Yang, C.; Hashimoto, K. Chem Mater 2009, 21, 4055–4061.

18 Wen, S. P.; Pei, J. N.; Zhou, Y. H.; Xue, L. L.; Xu, B.; Li, Y. W.; Tian, W. J. J Polym Sci Part A: Polym Chem 2009, 47, 1003–1012.

19 Peng, Q.; Xu, J.; Zheng, W. J Polym Sci Part A: Polym Chem 2009, 47, 3399–3408.

20 Chang, Y.-T.; Hsu, S.-L.; Su, M.-H.; Wei, K.-H. Adv Funct Mater 2007, 17, 3326–3331.

21 Chang, Y.-T.; Hsu, S.-L.; Chen, G.-Y.; Su, M.-H.; Singh, T. A.; Diau, E. W.-G.; Wei, K.-H. Adv Funct Mater 2008, 18, 2356–2365.

22 Chang, Y.-T.; Hsu, S.-L.; Su, M.-H.; Wei, K.-H. Adv Mater 2009, 21, 2093–2097.

23 Cravino, A.; Sariciftci, N. S. J Mater Chem 2002, 12, 1931–1943.

24 Giacalone, F.; Segura, J. L.; Martin, N.; Gatellani, M.; Luzzati, S.; Lupsac, N. Org Lett 2003, 5, 1669–1672.

25 Tan, Z.; Hou, J.; He, Y.; Zhou, E.; Yang, C.; Li, Y. Macromolecules 2007, 40, 1868–1873.

26 Koyuncu, S.; Zafer, C.; Koyuncu, F. B.; Aydin, B.; Can, M.; Sefer, E.; Ozdemir, E.; Icli, S. J Polym Sci Part A: Polym Chem 2009, 47, 6280–6291.

27 Struijk, C. W.; Sieval, A. B.; Dakhorst, J. E. J.; van Dijk, M.; Kimkes, P.; Koehorst, R. B. M.; Donker, H.; Schaafsma, T. J.; Picken, S. J.; van de Craats, A. M.; Warman, J. M.; Zuilhof, H.; Sudhölter, E. J. R. J Am Chem Soc 2000, 122, 11057–11066.

28 Jones, B. A.; Facchetti, A.; Wasielewski, M. R.; Marks, T. J. J Am Chem Soc 2007, 129, 15259–15278.

29 Hüttner, S.; Sommer, M.; Thelakkat, M. Appl Phys Lett 2008, 92, 093302.

30 Yan, H.; Zheng, Y.; Blache, R.; Newman, C.; Lu, S. F.; Woerle, J.; Facchetti, A. Adv Mater 2008, 20, 3393–3398.

31 Neuteboom, E. E.; Meskers, S. C. J.; van Hal, P. A.; van Duren, J. K. J.; Meijer, E. W.; Janssen, R. A. J.; Dupin, H.; Pourtois, G.; Cornil, J.; Lazzaroni, R.; Brédas, J.-L.; Beljonne, D. J Am Chem Soc 2003, 125, 8625–8638.

32 Sommer, M.; Lindner, S. M.; Thelakkat, M. Adv Funct Mater 2007, 17, 1493.

33 Zhan, X. W.; Tan, Z.; Domercq, B.; An, Z.; Zhang, X.; Barlow, S.; Li, Y. F.; Zhu, D. B.; Kippelen, B.; Marder, S. R. J Am Chem Soc 2007, 129, 7246–7247.

34 Hua, J. N.; Lam, J. W. Y.; Yu, X. M.; Wu, L. J.; Kwok, H. S.; Wong, K. S.; Tang, B. Z. J Polym Sci Part A: Polym Chem 2008, 46, 2025–2037.

35 Zhang, Q.; Cirpan, A.; Russell, T. P.; Emrick, T. Macromolecules 2009, 42, 1079–1082.

36 Rajaram, S.; Armstrong, P. B.; Kim, B. J.; Fréchet, J. M. J Chem Mater 2009, 21, 1775–1777.

37 Neuteboom, E. E.; van Hal, P. A.; Janssen, R. A. J. Chem Eur J 2004, 10, 3907–3918.

38 Chen, L. X.; Xiao, S.; Yu, L. J Phys Chem B 2006, 110, 11730–11738.

39 Bauer, P.; Wietasch, H.; Lindner, S. M.; Thelakkat, M. Chem Mater 2007, 19, 88–94.

40 Koyuncu, S.; Kus, M.; Demic, S.; Kaya, I.; Ozdemir, E.; Icli, S. J Polym Sci Part A: Polym Chem 2008, 46, 1974–1989.

41 Morin, J.-F.; Drolet, N.; Tao, Y.; Leclerc, M. Chem Mater 2004, 16, 4619–4626.

42 Kobayashi, N.; Koguchi, R.; Kijima, M. Macromolecules 2006, 39, 9102–9111.

43 Grigalevicius, S.; Ma, L.; Xie, Z.-Y.; Scherf, U. J Polym Sci Part A: Polym Chem 2006, 44, 5987–5994.

44 Xie, L.-H.; Deng, X.-Y.; Chen, L.; Chen, S.-F.; Liu, R.-R.; Hou, X.-Y.; Wong, K.-Y.; Ling, Q.-D.; Huang, W. J Polym Sci Part A: Polym Chem 2009, 47, 5221–5229.

45 Blouin, N.; Michaud, A.; Leclerc, M. Adv Mater 2007, 19, 2295–2300.

46 Wakim, S.; Beaupré, S.; Blouin, N.; Aich, B.-R.; Rodman, S.; Gaudiana, R.; Tao, Y.; Leclerc, M. J Mater Chem 2009, 19, 5351–5358.

47 Park, S. H.; Roy, A.; Beaupré, S.; Cho, S.; Coates, N.; Moon, J. S.; Moses, D.; Leclerc, M.; Lee, K.; Heeger, A. J Nat Photonics 2009, 3, 297–302.

48 Zhang, M.; Tsao, H. N.; Pisula, W.; Yang, C.; Mishra, A. K.; Müllen, K. J Am Chem Soc 2007, 129, 3472–3473.

49 Morana, M.; Wegscheider, M.; Bonanni, A.; Kopidakis, N.; Shaheen, S.; Scharber, M.; Zhu, Z.; Waller, D.; Gaudiana, R.; Brabec, C. Adv Funct Mater 2008, 18, 1757–1766.

50 Zhu, Z.; Waller, D.; Gaudiana, R.; Morana, M.; Mühlbacher, D.; Scharber, M.; Brabec, C. Macromolecules 2007, 40, 1981–1986.

51 Lee, J. K.; Ma, W. L.; Brabec, C. J.; Yuen, J.; Moon, J. S.; Kim, J. Y.; Lee, K.; Bazan, G. C.; Heeger, A. J. J Am Chem Soc 2008, 130, 3619–3623.

52 Li, K.-C.; Hsu, Y.-C.; Lin, J.-T.; Yang, C.-C.; Wei, K.-H.; Lin, H.-C. J Polym Sci Part A: Polym Chem 2009, 47, 2073–2092.

53 Brédas, J.-L.; Beljonne, D.; Coropceanu, V.; Cornil, J. Chem Rev 2004, 104, 4971–5004.

54 Scharber, M. C.; Mühlbacher, D.; Koppe, M.; Denk, P.; Waldauf, C.; Heeger, A. J.; Brabec, C. J Adv Mater 2006, 18, 789–794.

55 Thompson, B. C.; Fréchet, J. M. J Angew Chem Int Ed 2008, 47, 58–77.

56 Freeman, A. W.; Urvoy, M.; Criswell, M. E. J Org Chem 2005, 70, 5014–5019.

57 Guo, X.; Watson, M. D. Org Lett 2008, 10, 5333–5336.

58 Brzeziński, J. Z.; Reynolds, J. R. Synthesis 2002, 8, 1053–1056.

59 Coppo, P.; Cupertino, D. C.; Yeates, S. G.; Turner, M. L. Macromolecules 2003, 36, 2705–2711.

60 Asawapirom, U.; Scherf, U. Macromol Rapid Commun 2001, 22, 746–749.

61 Cremer, L. D.; Vandeleene, S.; Maesen, M.; Verbiest, T.; Koeckelberghs, G. Macromolecules 2008, 41, 591–598.

62 Bonnet, J. P.; Tran-Van, F.; Chevrot, C. Synth Met 2006, 156, 1292–1298.

63 Lav, T.-X.; Tran-Van, F.; Bonnet, J.-P.; Chevrot, C.; Peralta, S.; Teyssié, D.; Grazulevicius, J. V. J Solid State Electrochem 2007, 11, 859–866.

64 Pommerehne, J.; Vestweber, H.; Guss, W.; Mahrt, R. F.; Bässler, H.; Porsch, M.; Daub, J. Adv Mater 1995, 7, 551–554.

65 Goh, C.; Kline, R. J.; McGehee, M. D.; Kadnikova, E. N.; Fréchet, J. M. J. Appl Phys Lett 2005, 86, 122110.

66 Ballantyne, A. M.; Chen, L.; Dane, J.; Hammant, T.; Braun, F. M.; Heeney, M.; Duffy, W.; McCulloch, I.; Bradley, D. D. C.; Nelson, J. Adv Funct Mater 2008, 18, 2373–2380.

67 Markov, D. E.; Hummelen, J. C.; Blom, P. W. M.; Sieval, A. B. Phys Rev B 2005, 72, 045216.

68 Kietzke, T.; Hörhold, H.-H.; Neher, D. Chem Mater 2005, 17, 6532–6537.